Combining Microsolvation and Polarizable Continuum Studies: New Insights in the Rotation Mechanism of Amides in Water

Clarissa O. da Silva,[†] Benedetta Mennucci,*[,‡] and Thom Vreven[§]

Departamento de Química, Universidade Federal Rural do Rio de Janeiro, BR456 km 47, Rio de Janeiro, Brazil, Dipartimento di Chimica e Chimica Industriale, Universitá degli Studi di Pisa, via Risorgimento 35, Pisa, Italy, and Gaussian Inc., 140 Washington Avenue, North Haven, Connecticut 06473

Received: March 18, 2003; In Final Form: June 3, 2003

We present a quantum mechanical investigation of the rotation mechanisms of *N*,*N*-dimethylformamide (DMF) and *N*,*N*-dimethylacetamide (DMA) in water. This rotation can happen through two distinct transition states known as TS1 and TS2, where the nitrogen lone pair is on the opposite side of the oxygen atom or on the same side, respectively. The analysis is focused on complementary descriptions of the solvent, either represented by a limited number of explicit solvent molecules (microsolvation), by an implicit (or continuum) solvation, or by combinations of these two approaches. The combined approach (microsolvation + continuum) can provide quantitative agreement with the experimental results for the gas to solution shift of the rotational barrier. For both amides, continuum effects alone are sufficient to select the correct channels. However, hydrogen-bond effects (via the explicit solvent molecules) are necessary to obtain quantitative agreement with experiment, provided this is combined with a continuum description. In the rotation in DMF, it seems that a single water molecule is directly involved, while the other solvent molecules act as a "mean field" (the bulk), which is well reproduced by a polarizable continuum medium. The mechanism in DMA is less clear. In gas phase the steric repulsive interactions between methyl groups make TS1 clearly favored with respect to TS2. In water, the larger dipole moment of TS2 produces an opposite effect with respect to the repulsion interactions, making the corresponding channel less disfavored than in gas phase. The results are compared with previous Monte Carlo simulations, and this comparison is used to draw a more general picture about how different descriptions of the solvent can take into account long-range and mediated effects on one side and shorter-range and dynamic effects on the other side.

1. Introduction

The inclusion of solvation effects in the computational modeling of chemical reactivity and processes has in some ways become a standard procedure. This does, however, not mean that including solvation effects is easy, neither that the definition of the best description is straightforward. The large variety of techniques in use ranges from representation of the solvent by a macroscopic (polarizable) continuum that surrounds the solute to the explicit incorporation of many solvent molecules. Despite their proven usefulness, each of the approaches currently in use has its particular weaknesses. For example, the electronic aspects of hydrogen bonding between solvent and solute is described poorly by continuum models, while explicit descriptions, which are always size-limited, cannot fully take into account long-range (or bulk) effects. It follows that many of the approaches complement each other, and it is therefore worthwhile to investigate the possibility of combining different techniques in the same calculation. This has indeed been the topic of a number of recent studies[1−5] in which the analysis is focused on complementary representations of the solvent, namely, explicitly by a small number of solvent molecules (microsolvation) or implicitly by a continuum, or by their combination. However, there are a number of important but not clearly evident issues that arise from such studies. In this work we will discuss several of these aspects, specifically those that arise when a quantum-mechanical (QM) microsolvation augmented with a polarizable continuum is used for the study of the central bond rotations of *N*,*N*-dimethylformamide (DMF) and *N*,*N*-dimethylacetamide (DMA) in aqueous solution.

DMF and DMA serve as prototypes for a number of biochemically important processes. Some binding proteins of the immunosuppressive agents cyclosporin A and rapamycin are classified as rotamases (peptidyl−prolyl cis/trans isomerases), because their action on the substrate happens through bond rotation processes.[6,7] The binding sites of these proteins are rich with hydrophobic residues, and their activity is retarded in polar solvents,[8] which suggests a relatively nonspecific mode of catalysis. Furthermore, DMF and DMA are commonly used as prototype compounds for the study of cis/trans isomerization about peptide bonds. Insights into their rotation mechanism can also bring more light to the understanding of protein folding in general. For these reasons, the rotation mechanisms of DMA and DMF have been the topic of various theoretical studies,[9−14] employing a variety of methodologies such as Monte Carlo[10,11] and high level ab initio calculations.[9,12] It was found that the equilibrium structures of both compounds have a planar O−C−N−$(C)_2$ moiety, as shown in Figure 1. The planarity of these systems can be understood if the π orbital of the C−O bond and the p pure orbital of the N atom are considered. When the molecule assumes a planar configuration, the system is stabilized

[†] Departamento de Química, UFRuralRJ. E-mail clarissa-dq@ufrrj.br.
[‡] Universitá degli Studi di Pisa. E-mail bene@dcci.unipi.it.
[§] Gaussian Inc. E-mail thom@Gaussian.com.

10.1021/jp0346918 CCC: $25.00
Published on Web 08/06/2003

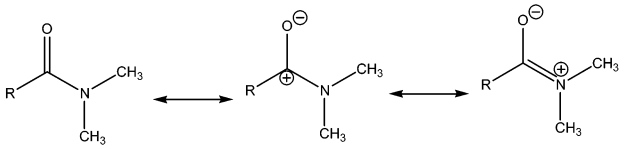

Figure 1. Resonance structures for the GS of the prototype amides.

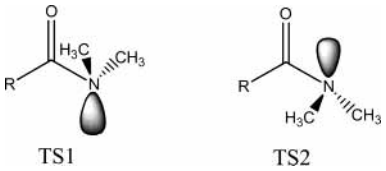

Figure 2. Rotational transition structures for DMF (R═H) and DMA (R═CH_3).

by the resulting conjugation,[15] which can be represented by the resonance structures in Figure 1.

Simultaneous rotation about the C−N bond and pyramidalization of the nitrogen atom leads to two different transition states, which are shown in Figure 2. In the first case, the nitrogen lone pair is on the opposite side of the oxygen atom (anti or trans, Figure 2), and in the second case the oxygen lone pair is on the same side (syn or cis, Figure 2). In this work, we refer to the transition structures as TS1 and TS2, respectively.

The literature agrees on the preferred channel for the C−N rotations in gas phase. For DMF both TS1 and TS2 are possible, while in DMA the repulsion between the methyl groups causes TS1 to be the only channel.[9] When the same process is studied in solution, however, the situation is less clear, and there is no agreement in the literature. Due to their different conformations, the transition structures have very different dipole moments and interact differently with solvents that have high dielectric constants. The situation becomes even less clear if a protic polar solvent as water is considered. Not only the bulk effects will be present but also specific interactions such as hydrogen bonds will be established between the amide and the solvent, and these could stabilize structures that are not energetically favored in gas phase or in other solvents.

Wiberg et al.[9] performed NMR selective inversion−recovery experiments on DMA and DMF and found that the heights of the C−N rotational barriers in aqueous solution are approximately 2.8 kcal/mol (for DMF) and 3.7 kcal/mol (for DMA) larger than the experimental values in a vacuum. They also carried out computational studies on the DMF and DMA rotations in gas phase and a variety of solvents, using an ab initio description coupled to the isodensity polarizable continuum model (IPCM).[16] Their theoretical studies found that, in water, the C−N rotation occurs through the same mechanisms as proposed for the gas phase: TS1 for DMA and a competition of both TS1 and TS2 for DMF.

Gao[10] studied the C−N rotation in DMF using a combined quantum mechanical and molecular mechanical (QM/MM) potential in Monte Carlo (MC) simulations. In this study it was found that in aqueous solution TS2 becomes the preferred transition state due to its higher dipole moment. Relative to the ground state, the solvation effect increases the activation free energy for TS1 by 2.7 ± 0.2 kcal/mol, while the change for TS2 is only 0.5 ± 0.1 kcal/mol. This results in barriers of 22.5 ± 0.2 and 20.8 ± 0.1 kcal/mol for TS1 and TS2, respectively.

Duffy et al.[11] investigated the effects of solvation on the free energies of activation for rotation about the carbonyl C−N bond in DMA, through a combination of gas-phase ab initio calculations and solution-phase statistical mechanics simulations (MC). They found that TS2 becomes competitive with TS1 in aqueous solution, because the former is stabilized by approximately 1.8 kcal/mol relative to the ground state, while TS1 is destabilized with respect to the ground state by approximately 2.1 kcal/mol. However, TS1 remains the favored channel, by about 0.2 ± 0.1 kcal/mol, with barriers of 16.71 and 16.91 kcal/mol for TS1 and TS2, respectively. The authors attribute the large stabilization of TS2 mainly to hydrogen-bond interactions between the oxygen and/or nitrogen of DMA and the hydrogen atoms of the solvent.

To summarize, there is no full agreement in the literature about the effect of solvation on the rotational mechanism of DMF and DMA prototypes in aqueous solution. In the present study we investigate this mechanism, using QM microsolvation of the solute combined with a continuum, as outlined in the next section.

2. Methodology

In this paper we apply the following combinations of microsolvation and a continuum description of the solvent.

Model 1: Gas Phase. The mechanism will be described in the gas phase. At this stage, we primarily want to evaluate the level of theory required by comparing our results to those accepted in the literature.

Model 2: Microsolvation. The calculation will still be carried out in gas phase, but one or two explicit water molecules are added to the GS and TS structures of DMA and DMF. In this model, the hydrogen-bond specific interactions are the main stabilizing factors.

Model 3: Continuum Solvent. The systems will be studied in aqueous solution with a solvent continuum description. In this model we do not include any specific solute−solvent interaction.

Model 4: Microsolvation and Continuum. Models 2 and 3 are combined. The clusters consisting of an amide plus one or two water molecules will be studied in a dielectric continuum, to analyze the effects of specific interactions coupled to the bulk effects.

In all the calculations we used the B3LYP functional with the basis set developed by Rablen et al.[17,18] to describe hydrogen-bonded complexes. The latter is a standard Pople basis set augmented by a set of diffuse polarization functions, included only on atoms that have lone pairs (N and O) with exponents one-fourth of that in the original set. In the following this basis set will be indicated as 6-31+G(d(X+),p). For the water molecules in the solute−solvent clusters we employed the 6-31+G(d,p) basis set.

For the continuum description of the solvent, we used the integral equation formalism (IEF)[19] version of the polarizable continuum model (PCM).[20,21] In this approach the solute is represented as a quantum mechanical charge distribution inside a cavity of molecular shape immersed in a macroscopic dielectric with known permittivity ϵ. The electrostatic interactions between solute and solvent can then be represented in terms of an apparent surface charge on the cavity, which produces a perturbation to the solute wave function, translated as an operator to be added to the solute Hamiltonian. The solution of the resulting quantum mechanical problem gives the solute wave function modified by the solvent in a mutually polarized way.

The molecular cavities were built from interlocking spheres centered on selected atoms, namely, all the carbons, the nitrogen, the oxygen, and for DMF, the hydrogen bonded to the carbonyl C; the radii of the corresponding spheres are 2.04 Å for the carbonyl C, 2.40 Å for the methyl carbons, 1.86 Å for N, 1.82 Å for O, and 1.44 Å for H in DMF (these values have been

TABLE 1: B3LYP/6-31+G(d(X+),P) Geometrical Parameters for Ground and Transition States of DMF in Gas Phase[a]

	GS calc	GS exp[27]	TS1 calc	TS2 calc
C═O	1.225	1.224	1.209	1.204
C−H	1.106	$(1.112)_{mean}$	1.106	1.117
C−N	1.362	1.391	1.441	1.436
N−C2[b]	1.451	$(1.453)_{mean}$	1.473	1.471
N−C1[b]	1.455	$(1.453)_{mean}$	1.473	1.471
NCO	125.6	123.5	125.1	124.4
C1NC	121.8	$(121.6)_{mean}$	110.9	109.5
C2NC	120.5	$(121.6)_{mean}$	111.0	109.5
θ(C2NCO)	180.0		62.4	118.9

[a] Distances are given in angstroms, and angles are given in degrees. [b] C1 and C2 refer to the two methyl carbons bonded to N.

TABLE 2: B3LYP/6-31+G(d(X+),P) Geometrical Parameters for Ground and Transition States of DMA in Gas Phase[a]

	GS calc	GS exp[b]	TS1 calc	TS2 calc
C═O	1.232	1.22	1.213	1.210
C−C	1.523	1.52	1.507	1.519
C−N	1.374	1.38	1.456	1.451
N−C2[c]	1.457	1.47	1.471	1.464
N−C1[c]	1.453	1.47	1.471	1.464
NC═O	121.8	122	122.6	120.2
C1NC	125.3	120	110.5	113.3
C2NC	119.5	120	110.5	113.2
θ(C2NC═O)	180.0		61.8	115.1

[a] Distances are given in angstroms, and angles are given in degrees. [b] Results of electron diffraction for *N*-methylacetamide,[28] since gas-phase data do not appear to be available for DMA. [c] C1 and C2 refer to the two methyl carbons bonded to N.

obtained by scaling the van der Waals radii[22] by a factor of 1.2). The explicit water molecules in the supermolecules are in cavities with spheres of radii 1.44 and 1.82 Å for H and O, respectively. Since the PCM-IEF quantum mechanical results include only electrostatic interactions, we added cavitation, dispersion, and repulsion terms in order to obtain free energies. These terms, referred to as nonelectrostatic contributions (NE), were computed by applying semiempirical formula based on the cavity surface and on solvent macroscopic parameters; for cavitation a generalization of a theory reducing the fluids to rigid classical bodies was used (see refs 23 and 24 for more details) while for dispersion and repulsion an approach based on the use of classical pair potentials projected on the cavity surface was adopted (see ref 25 for details). Throughout this work, the geometries were optimized for the respective level of theory. All the calculations were performed with a private development version of the Gaussian computational code.[26]

3. Numerical Results

3.1. Model 1: Gas Phase. In Tables 1 and 2 we report a selection of B3LYP/6-31+g(d(X+),p) geometrical data for DMF and DMA in gas phase, compared with available experimental data.[27,28] Upon rotation to the transition states, the most significant structural changes are the nitrogen pyramidalization and the C−N bond elongation. For both amides, the difference between the C═O and C−N distances is smaller in the GS than in the TS, which shows that the rotation reduces the π space interaction between O and N. The main geometrical differences between DMF and DMA are in the C1NC and C2NC angles. In DMF the two angles are very similar in the GS, while in DMA the methyl−methyl repulsion causes them to be quite different. In addition, in TS2 the C1NC and C2NC angles for DMF and DMA are 109.5° and 113.3°, respectively, which again can be attributed to repulsive effects between methyl groups.

TABLE 3: Height of the Rotational Barrier for the C−N Bond in DMA and DMF in Gas Phase[a]

	DMF				DMA			
	TS1		TS2		TS1		TS2	
	ΔE	ΔG	ΔE	ΔG	ΔE	ΔG	ΔE	ΔG
this work	22.77	**22.43**	22.30	**21.75**	16.83	**17.38**	19.96	19.90
ref 4[b]	19.54	20.07	19.44	19.64	15.05	15.64	18.05	18.13
ref 5[c]	19.87	19.80	20.46	20.24				
ref 6[c]					14.32	14.61	18.55	18.71
exp[29]	19.25; 19.4 ± 0.1				15.3 ± 0.1			

[a] Rotational barrier values are given in kilocalories per mole. [b] G2(MP2) level. [c] MP4(SDTQ)/6-31g(d).

We note the good agreement between the experimental data and the calculated parameters obtained with a B3LYP/6-31+g(d(X+),p) for the GS of both amides. This confirms the reliability of the level of theory for the GS. Since experimental data are not available for the transition states, we can only compare our results to previous theoretical work; the agreement remains satisfactory.[9,12]

In Table 3, we report our calculated gas-phase rotational barriers over the C−N bond, compared to experimental data and previous theoretical results. All the computed free energy data ΔG include both zero-point energy (ZPE) and thermal and entropic corrections to 298.15 K. The thermal corrections are obtained by assuming both the harmonic approximation for all vibrations and the rigid rotor model for all rotations. We see that our values for the barrier heights are higher than experimental and previously reported theoretical values. This can be related to the B3LYP hybrid functional, despite it being used with a basis set optimized for these types of systems.[17] However, the differences between the TS1 and TS2 barrier heights (0.68 kcal/mol for DMF and 2.52 kcal/mol for DMA) are very close to those computed by Wiberg et al. (0.43 and 2.49 kcal/mol), which represent the most accurate results to date. Since in this work we are mainly interested in the relative barrier heights, which B3LYP/6-31+G(d(X+),p) predicts accurately, we have continued using this level of theory.

Our theoretical description clearly identifies TS1 as the transition structure for the rotation of DMA, in accordance with the previous works. For DMF, however, it is not possible to identify TS1 or TS2 as the preferred channel as the heights of the barriers are very similar. Therefore, we can only say that both channels are possible reaction paths for the C−N rotation of DMF in gas phase. As suggested by Wiberg et al.,[9] it is in this case important to consider that a part of the reaction will proceed via the energetically slightly higher transition state. Therefore an *effective free energy* is introduced, which applies the Arrhenius formula assuming that the rate constants of the individual channels can be summed to give the total rate constant. For DMF the effective $\Delta G^{\ddagger}$ is 21.58 kcal/mol. For DMA, where the two channels are well separated, the resulting effective $\Delta G^{\ddagger}$ is identical to the height of the TS1, the lowest of the two barriers. In Table 3, values shown in boldface type are those that significantly contribute to the effective $\Delta G^{\ddagger}$.

3.2. Model 2: Computing H-Bond Interactions. Since previous Monte Carlo studies[10,11] showed that oxygen is the most effective site for hydrogen bonding, we started the geometry optimizations of the amide + water clusters from O---H structures. Three different sets of clusters were considered, which are schematically represented in Figure 3. Since the DMF and DMA clusters are very similar, we show only

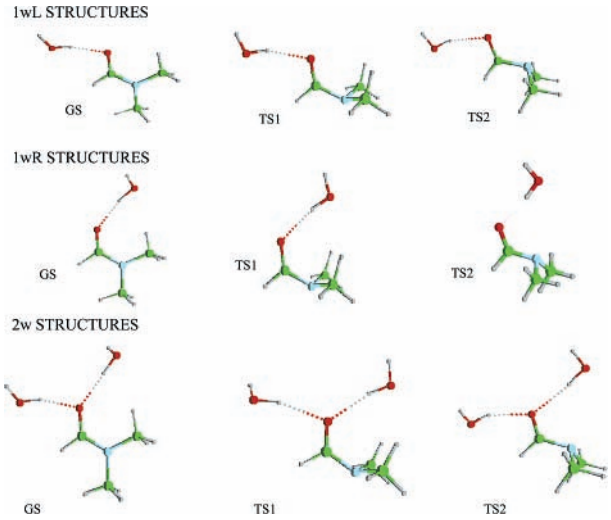

Figure 3. Scheme of the clusters of DMF + water considered in the calculations.

TABLE 4: (C)O--HOH Distances[a] in the Gas-Phase Complexes

		GS	TS1	TS2
DMF	1wR	1.877	1.954	2.038
	1wL	1.865	1.955	1.952
	2w	1.886 (L)	1.980 (L)	1.996 (L)
		1.886 (R)	1.993 (R)	2.094 (R)
DMA	1wR	1.865	1.921	2.038
	1wL	1.841	1.922	1.914
	2w	1.868 (L)	1.952 (L)	1.964 (L)
		1.896 (R)	1.955 (R)	1.995 (R)

[a] Distances are given in angstroms.

the former. In set 1, called 1wL, one water molecule is hydrogen-bonded to the carbonyl oxygen, located opposite (left) the amino group in both the GS and in the TS structures. In set 2, 1wR, the water molecule is located on the same side (right) with respect to the amino group. Finally set 3, 2w, combines sets 1 and 2.

The geometrical arrangement of the amides in the clusters is very similar to those without water molecules, in Tables 1 and 2, and is not reported here. The hydrogen-bond distances in the clusters are shown in Table 4. The increase in O---H distances going from GS to TS1 and TS2 indicates that the C−N rotation reduces the hydrogen-bond strengths. This was observed in Monte Carlo simulations as well.[11] Due to the inductive effect of the methyl group, DMA has stronger hydrogen-bond interactions than DMF. Indeed, all the corresponding ∼C═O---HOH distances are shorter for DMA than for DMF.

For both amides, the hydrogen-bond lengths differ significantly between TS1 and TS2 in the 1wR clusters, while they are very similar in the 1wL clusters. These findings, together with the fact that in the 1wL-TS2 structures the H-bond is significantly shorter than it is in 1wR-TS2, may be an indication that the ∼C═O---HOH interaction is less strong at the right side of the molecule. This is most likely due to the presence of the lone pair on nitrogen, which also explains why the perturbation is larger in DMA in which the amino group shows a more pronounced donorlike behavior.[15]

Passing on to the energetics, it is interesting to first comment on the relative stabilities of the clusters in their TS conformations. For TS1, the 1wL structure is always more stable than the 1wR structure (by 0.4 kcal/mol for both amides). In case of TS2 this is only true for DMF, for which 1wL is more stable by 1 kcal/mol; for DMA the two structures are nearly identical in energy.

TABLE 5: Height of the C−N Rotational Barrier for Clusters of DMA and DMF plus Water in Gas Phase[a]

	DMF				DMA			
	TS1	TS2	eff $\Delta G^{\ddagger}$	$\Delta\Delta G^{\ddagger}$	TS1	TS2	eff $\Delta G^{\ddagger}$	$\Delta\Delta G^{\ddagger}$
1wR	24.29	**22.67**	22.67	1.09	**19.40**	**20.44**	**19.30**	1.92
1wL	24.57	**22.92**	22.92	1.34	**18.36**	20.44	18.36	0.98
2w	25.08	**22.34**	22.34	0.76	**19.63**	**21.04**	**19.58**	2.20
exp[9]		22.04		2.79		19.05		3.85

[a] Rotational barrier values are given in kilocalories per mole; ZPE + themal corrections are included.

In Table 5 we report the rotational barriers for the clusters. As in Table 3, values shown in boldface type are those that significantly contribute to the effective $\Delta G^{\ddagger}$. When the heights for the TS1 and TS2 barriers are very different, the effective $\Delta G^{\ddagger}$ is determined by the lowest energy channel. As shown earlier for the gas-phase calculations, our level of theory overestimates the rotational barriers.[9] Therefore we introduce $\Delta\Delta G^{\ddagger} = \Delta G^{\ddagger}(\mathrm{X}) - \Delta G^{\ddagger}(\text{model 1})$, where X = 1wR, 1wL, or 2w. This quantity represents the shift of the barrier going from gas phase to solvated phase, which we can compare between experiment and our cluster models. Note that the experimental $\Delta\Delta G^{\ddagger}$ is not the shift from gas phase to mono- or dihydrated clusters, as in our model 2 calculations, but the shift from gas phase to *fully solvated* phase.

From results of Table 5 we see that for DMF the water molecules preferentially stabilize the TS2 structures. Since the isolated systems TS1 and TS2 are very close in energy (see Table 3), TS2 now becomes the preferred channel. This corresponds qualitatively to the trend observed in MC simulations. Our calculations give an average shift of +2 kcal/mol for TS1 and less than +1 kcal/mol for TS2, while MC calculations predict 2.7 and 0.5 kcal/mol, respectively. However, the agreement with experiment is poor. None of the considered clusters calculations reproduces the increase in barrier height of 2.79 kcal/mol, with 1wL (1.34 kcal/mol) yielding the shift closest to experiment.

For DMA the analysis is slightly more complex. From the results reported in Table 5, it follows that the presence of a water molecule at the right side of the carbonyl (1wR, 2w) stabilizes the TS2 structure. This makes the two transition states competitive, though TS1 remains the preferred channel. On the contrary, a single water molecule on the left (1wL) yields the same barriers as the isolated system, and TS1 remains the only possible channel. Data from MC simulations predicts that both channels are possible, with a gas-to-solution shift of about 2.2 kcal/mol, which is very close to our 2w result. However, also for DMA there is not a quantitative agreement with the experimental shift. It is clear that inclusion of hydrogen-bond interactions via a small number of explicit water molecules cannot fully account for the solvent effect on the rotational barrier.

3.3. Model 3: Computing Bulk Effects. As an alternative to the microsolvation scheme described in the previous section, we now apply the PCM-IEF model for solvation. The geometrical changes upon rotation with PCM are similar but more pronounced, as observed in the gas-phase calculations. In Table 6 we report the PCM-IEF rotational barriers for DMF and DMA in water for both channels and the effective $\Delta G^{\ddagger}$ with the corresponding gas-to-solution shift ($\Delta\Delta G^{\ddagger}$). We also report experimental results, as well as theoretical results reported by

TABLE 6: Height of the Rotational Barriers in DMA and DMF in Water[a]

	DMF				DMA			
	TS1	TS2	eff $\Delta G^{\ddagger}$	$\Delta\Delta G^{\ddagger}$	TS1	TS2	eff $\Delta G^{\ddagger}$	$\Delta\Delta G^{\ddagger}$
this work	25.04	**22.76**	22.75	1.17	**19.59**	**19.84**	19.29	1.92
ref 9[b]	22.77	20.77	20.75	1.34	17.87	18.32	17.64	2.01
ref 10[c]	22.5 ± 0.2	20.7 ± 0.1	20.67	1.10[d]				
ref 11[c]					16.71	16.91	16.39	1.78[d]
exp[9,9]			22.04	2.79			19.05	3.85

[a] Rotational barrier values are given in kilocalories per mole. [b] IPCM. [c] Monte Carlo. [d] Such values were obtained from the difference between effective $\Delta G^{\ddagger}$ in solution and gas phase. The effective $\Delta G^{\ddagger}$ values for refs 10 and 11 were introduced here for the first time; gas-phase values are 19.57 kcal/mol for DMF and 14.61 kcal/mol for DMA.

TABLE 7: Dipole Moments of GS and TS of DMF and DMA in Gas Phase and in Water[a]

	DMF			DMA		
	GS	TS1	TS2	GS	TS1	TS2
Vac	4.253	1.943	3.508	4.045	2.085	3.641
PCM-IEF	5.877	2.487	4.767	5.757	2.780	5.148

[a] Dipole moments are given in debyes.

others. From the latter we derived the effective $\Delta G^{\ddagger}$ for comparison with the current results.

From results reported in Table 6 it follows that for DMF the TS2 channel is favored. Gao obtained the same result with a QM/MM MC approach, which confirms the ability of the continuum approach to accurately reproduce statistical explicit solvent models. However, just as in Gao's results and our results obtained with model 2, $\Delta\Delta G^{\ddagger}$ is still too small compared to the experimental values. For DMA, the channels are very close in energy and the resulting effective $\Delta G^{\ddagger}$ is smaller than that for either channel. Similar to DMF, the same results were obtained with MC simulations,[11] but also here the computed gas-to-solution shift is too small compared to experiment.

To further analyze the PCM-IEF results, we calculated the dipole moments of GS and the TSs, both in the gas phase and with continuum (Table 7). For both amides, TS1 has the smallest dipole moment, and as a consequence it is less stabilized in water than GS and TS2 are. This results in a gas-to-solution (positive) shift larger for TS1 than for TS2. For DMF this is reflected in the fact that, from the two possible channels found in gas phase, we pass to the clearly preferred TS2 in water. For DMA the picture is less clear. In gas phase the steric repulsion between the methyl groups makes TS1 clearly favored over TS2, but in water, the larger dipole moment of TS2 opposes the repulsive interactions. This ultimately results in computed barriers for TS1 and TS2 in water that are very similar.

From previous paragraphs it follows that the description obtained with the continuum-only model is qualitatively correct. Both the assignment of the most favored mechanism in the two amides and the estimation of the differential solvation effect (larger for DMA than for DMF) are correctly predicted. The reason for the prediction not being quantitative is the neglect of specific interactions between the amides and water. As indicated by the data in Table 5, hydrogen bonding occurs between the solute and solvent, which can significantly affect the height of the barriers.

3.4. Model 4: Computing both Specific Interactions and Bulk Effects. To improve the description of the solute−solvent interaction given by the continuum-only model, we now explicitly include several solvent molecules that may strongly interact with the solute. Recently this strategy was successfully applied in the prediction of properties of solvated systems,[4,29] but here we will use the approach to study the rotational barriers.

TABLE 8: (C)O···HOH Distances (in Å) in the PCM Clusters[a]

		GS	TS1	TS2
DMF	1wR	1.822	1.923	1.916
DMF	1wL	1.774	1.898	1.902
DMF	2w	1.808 (L)	1.930 (L)	1.927 (L)
		1.857 (R)	1.968 (R)	1.948 (R)
DMA	1wR	1.808	1.899	1.881
DMA	1wL	1.764	1.875	1.876
DMA	2w	1.822, 1.859	1.915, 1.936	1.909, 1.920

[a] Distances are given in angstroms.

TABLE 9: Height of the C−N Rotational Barrier for Clusters of DMA and DMF Plus Water in Aqueous Solution[a]

	DMF				DMA			
	TS1	TS2	eff $\Delta G^{\ddagger}$	$\Delta\Delta G^{\ddagger}$	TS1	TS2	eff $\Delta G^{\ddagger}$	$\Delta\Delta G^{\ddagger}$
1wR	27.05	**24.14**	24.14	2.56	**20.65**	**20.33**	19.85	2.47
1wL	26.36	**24.03**	24.03	2.45	**21.26**	**21.46**	20.94	3.56
2w	26.21	**22.82**	22.82	1.24	**22.15**	**21.47**	21.31	3.93
exp[9,9]		22.04		2.79		19.05		3.85

[a] Rotational barrier values are given in kilocalories per mole; ZPE + themal corrections are included.

In Table 8 we report geometrical parameters related to the hydrogen bonding of the amides with the water molecules. From the results in Tables 4 and 8, it follows that solvating the clusters enlarges the hydrogen-bond strength, as indicated by the contraction of (C)O···HOH distances with respect to the gas-phase clusters. Furthermore, the difference between 1wR and 1wL lengths is significantly increased.

In Table 9 we report the $\Delta G^{\ddagger}$ for the TS1 and TS2 channels in the DMF and DMA cluster-continuum calculations, with one and two hydrogen-bonded water molecules. For all systems we report the effective $\Delta G^{\ddagger}$ as well as the resulting $\Delta\Delta G^{\ddagger}$ shift. For DMF, we again find TS2 to give the lowest rotational barrier, exactly as found for the isolated clusters and the continuum-only descriptions and in agreement with the MC simulations by Gao. Now, however, we find much better quantitative agreement with experiment, but only for the 1wR and 1wL cluster-continuum models.

For DMA, the PCM calculations change the results obtained for gas-phase and isolated clusters. In all the clusters, the presence of a dielectric continuum makes the two barriers very close in energy, similar to the observation for the continuum scheme without explicit water molecules (model 3). In fact, TS2 is more stabilized by the solvent interactions than TS1, as was found by Duffy et al.[11] using a MC approach that includes both short- and long-range effects. This time we find very good agreement with experiment for the 1wL and 2w models.

3.5. Alternative Clusters. In the Monte Carlo studies on DMA and DMF by Gao and Duffy, it was reported that in the TS2 structures hydrogen bonding also occurs between the water

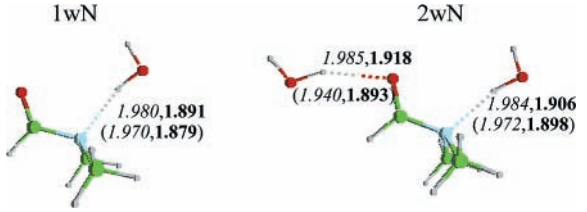

Figure 4. TS2 clusters with N---HOH hydrogen bond. Hydrogen-bond distances (in angstroms) are reported for DMF, and in parentheses for DMA, in a sequence of two numbers: the number in italic type is the length of hydrogen bond in model 2, and that in boldface type is the respective value in model 4.

TABLE 10: Free Energy Difference between the Two Possible TS2 Structures (1wR and 1wN) and (2w and 2wN)[a]

	gas phase		PCM	
	DMF	DMA	DMF	DMA
1w	0.7	0.2	0.9	0.2
2w	0.5	0.7	1.3	0.7

[a] Free energy is given in kilocalories per mole, with reference to the 1wN or 2wN cluster.

molecules and the nitrogen atom of the amino group. We investigated this possibility with the additional set of clusters shown in Figure 4. It is important to emphasize that N···HOH interaction can only be established when the water molecule is on the same side of the amino group, analogous to the 1wR and 2w clusters in the previous sections. The clusters obtained for DMF (for DMA they are equivalent) in Figure 4 will be referred to as 1wN and 2wN.

In Figure 4 we also report the H-bond distances for the TS2(N) clusters obtained in gas phase and with PCM. Comparing these data with those reported in Tables 4 and 8, we see that the hydrogen-bond lengths of the 1wR and 2w clusters (Tables 4 and 8) are longer than the corresponding distances in 1wN and 2wN, which indicates that hydrogen bonding with the N atom is stronger than with the O atom. Furthermore, from the geometrical data presented in this and the previous sections, it follows that adding the continuum enlarges the hydrogen-bond strength.

In Table 10 we report the free energy differences between the TS2(N) and the corresponding TS2(O) structures. All the TS2(N) structures are more stable than the corresponding TS2(O) structures, which is most pronounced in DMF with the continuum description of the solvent. Consideration of the N···HOH interaction, either as alternative (1wN) or additive to O···HOH (2wN), does not change the channel preferences obtained in the previous sections. TS2 is still the most probable, but in each case the shift in the barrier becomes too small compared to experiment. In fact, the gas to solution shift disappears for the DMF 2wN model.

3.6. Summary. In Figures 5 and 6 we present an overview of the results obtained with the different models. The GS is taken as the reference and the plot presents a zoom on the region around the TS barriers. The exp line is an estimate of the experimental barrier in water, which has been obtained by summing the experimental value of the barrier in solution and the error associated with the B3LYP description [defined as the difference between the B3LYP/6-31+G(d(X+),p) and the experimental gas-phase barriers]. We use this correction for the same reason as the use of the $\Delta\Delta G^{\ddagger}$ quantity in the previous sections.

When analyzing these plots, we must keep in mind that the preferred channel must satisfy two conditions. First there must be agreement with the experimental value, and second, that

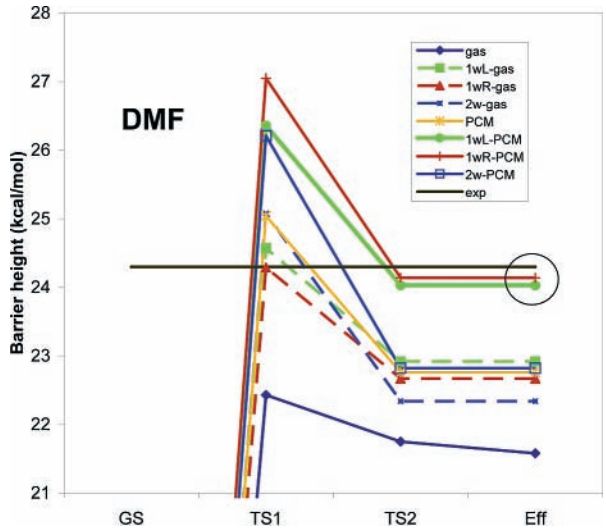

Figure 5. Representation of the TSs and effective rotational barriers for DMF in the various models considered.

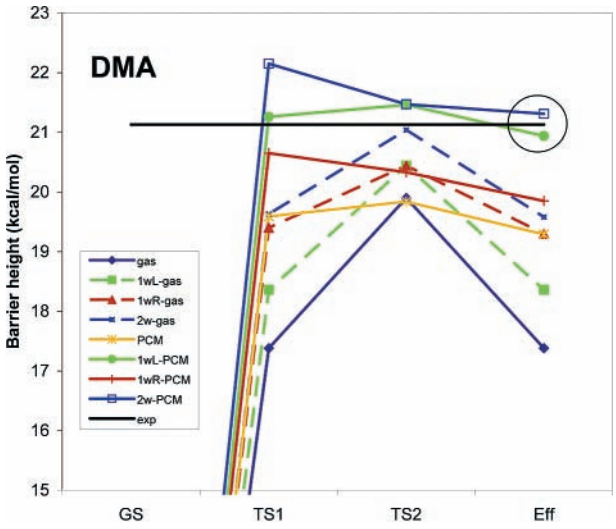

Figure 6. Representation of the TSs and effective rotational barriers for DMA in the various models considered.

channel must correspond to the lowest rotational barrier. As shown in Figure 5, for DMF the TS2 structure has always a smaller barrier than TS1. In the gas phase, the difference is only about 0.7 kcal/mol, and the effective barrier has both TS1 and TS2 contributions. Inclusion of solvent (models 2, 3, and 4) results in very distinct values for TS1 and TS2, and the effective barrier is identical to TS2 in all cases. From the 1wR-gas and 1wL-gas results it follows that when only one water molecule is added (1wX-gas), its effect on the height of the barrier is more or less independent of its location. There is, however, no agreement with the experimental value. Addition of a second water molecule (2w-gas) enlarges the TS1 and TS2 energy difference and leads to values far away from experiment. Inclusion of solvent via only the continuum (PCM) leads to results very similar to those for model 2, and this seems to show that H-bonding and bulk effects are quite similar for this system. This is confirmed by the results obtained with model 4, in which solvation effects are considered via both PCM and microsolvation. In this scheme, the 1w-PCM (L or R) TS2 structure satisfies both requirements for the preferred channel for DMF (the circled values in Figure 5).

In Figure 6 we show the equivalent plot for DMA, for which the results are less uniform than for DMF. In the isolated (gas-

phase) amide, TS1 is clearly favored over TS2. The 1w-gas or 2w-gas results show that inclusion of only the hydrogen-bond effects does not change the preference. With only the continuum description of the solvent, both transition structures become possible channels, which is also the case for the 1wL-PCM description. However, in the 1wR-PCM and 2w-PCM models, TS1 is more destabilized than TS2, although in each case both TS1 and TS2 contribute to the effective barrier. Just from looking at the absolute values for the height of the barrier (circled values), it is not possible to distinguish between 2w-PCM and 1wL-PCM results.

4. Conclusions

In the previous sections we have compared different solvation models to study the changes of the rotation mechanisms of DMF and DMA passing from gas phase to aqueous solution. In gas phase, the DMF rotation happens through both TS1 and TS2, but the same C−N rotation in DMA preferentially happens through a TS2 structure. This preference is due to the methyl−methyl steric repulsion. In aqueous solution, the situation is different. The two possible transition structures have very different dipole moments, which leads to distinct solute−solvent interactions. In DMF, TS2 is the preferred channel irrespective of the theoretical model. On the contrary, the preferred mechanism of DMA depends on the theoretical description of the solvent and can therefore be completely misunderstood if not all solvent effects are properly taken into account. When only specific hydrogen-bond interactions are considered (model 2), it is not straightforward to identify the operative channel for DMA. Conversely, when just the bulk effects are considered (model 3), the results are qualitatively in agreement with experiments. However, only when specific interactions and bulk effects are taken into account together (model 4) can we obtain quantitative agreement between theoretical and experimental values for the gas to solution shift in the respective rotational barrier.

The correlation between computed and experimental results allows us to propose the rotational mechanisms of the two amides in water solution. In the rotation in DMF, it appears that a single water molecule is directly involved, while the other solvent molecules act as a "mean field" (the bulk), which is well reproduced by a polarizable continuum medium. This water molecule can be indistinguishably located on the right or on the left to the carbonyl, following the results obtained from our approach.

The mechanism in DMA is less clear. Perhaps due to the inductive effect of the methyl group, the water molecule H-bonded to the carbonyl oxygen located on the right side of the amide (1wR and 2w) is more effectively perturbed by the nitrogen lone pair than in DMF. This increased stabilization of TS2, when the water molecule is on the right side, can cause TS2 to be preferred over TS1.

Some conclusive comments can now be sketched.

From this study it is evident that the results obtained with the continuum-only model are very close to the QM/MM MC results of refs 10 and 11 (same $\Delta\Delta G^{\ddagger}$ value and same differences between TS1 and TS2), while things are quite different for models with the explicit solvent molecules. The main reason for the agreement between MC and PCM is that in both the solvent is (statistically) averaged: in MC explicitly, and in PCM implicitly. In addition, in both PCM and QM/MM MC, the wave function "feels" the charge distribution of the solvent, in MC via the explicit point charges of the MM region, and in PCM via the charge distribution on the cavity surface. So, in that sense, MC and PCM are very similar and yield (when parametrized correctly) the same results quantitatively. PCM, however, is not able to get steric effects of the solvent right, but that appears not to be a problem here.

Both MC and PCM do not get specific interactions such as H-bonding right, and that, of course, is the problem in the present work. This limitation is here solved by introducing one or two water molecules in addition to the continuum description: this limited approach (one or two water plus continuum PCM) is not only able to account for the main solute−solvent interactions present in the systems studied but also furnishes a good quantitative agreement with the experimental results for the gas to solution shift of the rotational barrier.

There are however, two (paradoxical) issues that need to be addressed in order to fully appreciate the results.

First, for DMF we see that inclusion of one water molecule and PCM reproduces the experimental values accurately but that there is no longer agreement with experiment when a second water molecule is added. This seems surprising at first, since common sense says that inclusion of additional solvent molecules at a high theoretical level should not negatively affect the quantitative description. This reasoning, however, ignores the fact that while PCM provides an averaged description of the solvent, the QM solvent molecules introduce some instantaneous interactions that in reality may not occur or, in a statistical sense, not "often". Thus, inclusion of QM solvent molecules improves the description only when the added QM molecules are supposed to be coordinated to the solute with a significant resident time, in a dynamical context. It is clear that this is a problem in our approach when just one instantaneous configuration has to resemble a noninteger average number of hydrogen bonds, as in fact predicted by the Monte Carlo simulations of DMA.

Second, explicit incorporation of solvent molecules might facilitate different interactions in the different compounds along the reaction path. This can be an artifact of only a limited number of QM solvent molecules being available. In fact, a limited number of explicit solvent molecules also prevents the correct accounting for the continuous changes in the solvation shells along the reaction path. It is possible that this is the origin of the 1wN and 2wN results underestimating the barrier: an O−H interaction in the ground state is replaced by a much stronger O−N interaction in the transition state and this artificially lowers the TS barrier significantly.

The two aspects we have introduced here seem to require two opposite strategies: the first asks to reduce the number of explicit waters to those firmly (in a dynamical sense) tight to the reacting system, while the second requires to enlarge such number so as to include also molecules not directly interacting with the reacting system. In reality, this opposition is only apparent; the problem is that a standard quantum-mechanical description in which the first solvation shells are obtained as the minima of the corresponding potential energy surface is not the correct way to look at the problem. Solvation is an intrinsically dynamic long-range phenomenon, especially when coupled to a reactive process, and statistical concepts involving averaging and fluctuations from averages are thus necessary. In this paper we have tried to show that solvation QM models with few explicit solvent molecules can still be used, but only if the statistical aspect is also included, at least in its approximated version represented by continuum approaches.

We can thus conclude that QM microsolvation in combination with a continuum, even if surely does not represent the final answer (for example, it completely misses effects due to

fluctuations), still represents one of the most promising tools for treating solvation phenomena and processes requiring the level of accuracy that only full quantum mechanical approaches can give.

Acknowledgment. We thank Professor Jacopo Tomasi for helpful discussions and suggestions. C. O. da Silva thanks the Brazilian agencies FAPERJ and CNPq for the financial support.

References and Notes

(1) Mohamed, A. A.; Jensen, F. *J. Phys. Chem. A* **2001**, *105*, 3259.
(2) Sicinska, D.; Paneth, P.; Truhlar, D. G. *J. Phys. Chem. B* **2002**, *106*, 2708.
(3) Re, S.; Morokuma, K. *J. Phys. Chem. A* **2001**, *105*, 7185.
(4) (a) Mennucci, B.; Martinez, J. M.; Tomasi, J. *J. Phys. Chem. A* **2001**, *105*, 7287. (b) Mennucci, B. *J. Am. Chem. Soc.* **2002**, *124*, 1506.
(5) Rivelino, R.; Coutinho, K.; Canuto, S. *J. Phys. Chem. B* **2002**, *106*, 12317.
(6) Fischer, G.; Schmid, F. X. *Biochemistry* **1990**, *29*, 2205.
(7) Schreiber, S. L. *Science* **1991**, *251*, 283.
(8) Drakenberg, T.; Dahlqvist, K.-I.; Forsen, S. J. *J. Phys. Chem.* **1972**, *76*, 2178.
(9) Wiberg, K. B.; Rablen, P. R.; Rush, D. J.; Keith, T. A. *J. Am. Chem. Soc.* **1995**, *117*, 4261.
(10) Gao, J. *J. Am. Chem. Soc.* **1993**, *115*, 2930.
(11) Duffy, E. M.; Severance, D. L.; Jorgensen, W. L. *J. Am. Chem. Soc.* **1992**, *114*, 7535.
(12) Vassilev, N. G.; Dimitrov, V. S. *J. Mol. Struct.* (a) **1999**, *484*, 39; (b) **2000**, *522*, 37.
(13) Leis, J.; Karelson, M. *Comput. Chem.* **2001**, *25*, 171.
(14) Langley, C. H.; Allinger, N. L. *J. Phys. Chem. A* **2002**, *106*, 5638.
(15) Raos, G.; Bieli, P.; Tornaghi, E. *Int. J. Quantum Chem.* **1999**, *74*, 249, and references therein.
(16) Foresman, J. B.; Keith, T. A.; Wiberg, K. B.; Snoonian, J.; Frisch, M. J. *J. Phys. Chem.* **1996**, *100*, 16098.
(17) Rablen, P. R.; Pearlman, S. A.; Miller, D. A. *J. Am. Chem. Soc.* **1999**, *121*, 227.
(18) Rablen, P. R.; Miller, D. A.; Bullock, V. R.; Hutchinson, P. H.; Gorman, J. A. *J. Am. Chem. Soc.* **1999**, *121*, 218.
(19) Cancès, E.; Mennucci, B.; Tomasi, J. *J. Chem. Phys.* **1997**, *107*, 3032.
(20) Miertus, S.; Scrocco, E.; Tomasi, J. *Chem. Phys.* **1981**, *55*, 117.
(21) Cammi, R.; Tomasi, J. *J. Comput. Chem.* **1995**, *16*, 1449.
(22) Bondi, A. *J. Phys. Chem.* **1964**, *68*, 441.
(23) Pierotti, R. A. *Chem. Rev.* **1976**, *76*, 717.
(24) Claverie, P. In *Intermolecular Interactions: from Diatomics to Biomolecules*; Pullman, B., Ed.; Wiley: Chichester, U.K., 1978.
(25) Floris, F. M.; Tomasi, J.; Pascual-Ahuir, J. L. *J. Comput. Chem.* **1991**, *12*, 784.
(26) Frisch, M. J., et al. *Development Version*; Gaussian, Inc: Pittsburgh, PA, 2002.
(27) Schultz, G.; Hargittal, I. *J. Phys. Chem.* **1993**, *97*, 4966.
(28) Kitano, M.; Fukuyama, T.; Kughitsu, K. *Bull. Chem. Soc. Jpn.* **1973**, *46*, 384.
(29) Cappelli, C.; Mennucci, B.; da Silva, C. O.; Tomasi, J. *J. Chem. Phys.* **2000**, *112*, 5382.